



Article

# Synthesis and Biological Activity of Myricetin Derivatives Containing Pyrazole Piperazine Amide

Fang Liu, Xiao Cao, Tao Zhang, Li Xing, Zhiling Sun, Wei Zeng, Hui Xin and Wei Xue \*

National Key Laboratory of Green Pesticide, Key Laboratory of Green Pesticide and Agricultural Bioengineering, Ministry of Education, Center for R&D of Fine Chemicals of Guizhou University, Guiyang 550025, China; gs.liuf20@gzu.edu.cn (F.L.); gs.xcao20@gzu.edu.cn (X.C.); gs.zt21@gzu.edu.cn (T.Z.); gs.lxing21@gzu.edu.cn (L.X.); gs.zlsun22@gzu.edu.cn (Z.S.); gs.wzeng22@gzu.edu.cn (W.Z.); gs.hxin22@gzu.edu.cn (H.X.)

\* Correspondence: wxue@gzu.edu.cn

**Abstract:** In this paper, a series of derivatives were synthesized by introducing the pharmacophore pyrazole ring and piperazine ring into the structure of the natural product myricetin through an amide bond. The structures were determined using carbon spectrum and hydrogen spectrum high-resolution mass spectrometry. Biological activities of those compounds against bacteria, including *Xac* (*Xanthomonas axonopodis* pv. *Citri*), *Psa* (*Pseudomonas syringae* pv. *Actinidiae*) and *Xoo* (*Xanthomonas oryzae* pv. *Oryzae*) were tested. Notably, **D6** exhibited significant bioactivity against *Xoo* with an EC<sub>50</sub> value of 18.8 µg/mL, which was higher than the control drugs thiadiazole-copper (EC<sub>50</sub> = 52.9 µg/mL) and bismethiazol (EC<sub>50</sub> = 69.1 µg/mL). Furthermore, the target compounds were assessed for their antifungal activity against ten plant pathogenic fungi. Among them, **D1** displayed excellent inhibitory activity against *Phomopsis* sp. with an EC<sub>50</sub> value of 16.9 µg/mL, outperforming the control agents azoxystrobin (EC<sub>50</sub> = 50.7 µg/mL) and fluopyram (EC<sub>50</sub> = 71.8 µg/mL). In vitro tests demonstrated that **D1** possessed curative (60.6%) and protective (74.9%) effects on postharvest kiwifruit. To investigate the active mechanism of **D1**, its impact on SDH activity was evaluated based on its structural features and further confirmed through molecular docking. Subsequently, the malondialdehyde content of **D1**-treated fungi was measured, revealing that **D1** could increase malondialdehyde levels, thereby causing damage to the cell membrane. Additionally, the EC<sub>50</sub> value of **D16** on *P. capsici* was 11.3 µg/mL, which was superior to the control drug azoxystrobin (EC<sub>50</sub> = 35.1 µg/mL), and the scanning electron microscopy results indicated that the surface of drug-treated mycelium was ruffled, and growth was significantly affected.

**Keywords:** pyrazole; piperazine; myricetin; antifungal activity; SDH; *P. capsici*; *Phomopsis* sp.



**Citation:** Liu, F.; Cao, X.; Zhang, T.; Xing, L.; Sun, Z.; Zeng, W.; Xin, H.; Xue, W. Synthesis and Biological Activity of Myricetin Derivatives Containing Pyrazole Piperazine Amide. *Int. J. Mol. Sci.* **2023**, *24*, 10442. <https://doi.org/10.3390/ijms241310442>

Academic Editor: Roberta Galeazzi

Received: 30 May 2023

Revised: 13 June 2023

Accepted: 15 June 2023

Published: 21 June 2023



**Copyright:** © 2023 by the authors. Licensee MDPI, Basel, Switzerland. This article is an open access article distributed under the terms and conditions of the Creative Commons Attribution (CC BY) license (<https://creativecommons.org/licenses/by/4.0/>).

## 1. Introduction

Phytopathogenic fungi and bacteria pose significant hazards to crop growth and the quality of agricultural products, causing substantial economic losses [1,2]. Moreover, the prolonged utilization of conventional fungicides in the market has led to drug resistance of plant pathogens, resulting in recurring bacterial and fungal diseases in most plants [3–7]. In recent years, there has been a heightened emphasis on the ecological environment by the government, prompting researchers in this field to search for efficient, environmentally friendly, and non-polluting agricultural fungicides [8,9].

Flavonoids are a class of plant secondary metabolites found in various plant species, exhibiting complex and distinct structural types. Flavonoids, as known as a natural substance, possess a variety of beneficial physiological activities and are considered safe and widely available. Myricetin is a flavanol compound extracted from the bark and leaves of the Myricaceae plant. It is also found in many edible plants, including fruits and vegetables, as well as many herbs and teas [10–14]. Chemically, myricetin is referred to as 3,5,7,3',4',5'-hexahydroxyflavone and belongs to the class of myricetin flavonoids. It

has various biological activities such as antibacterial [15], antiviral [16,17], antioxidant [18] and hypoglycemic [19]. In addition, due to its planar structure and multiple phenolic hydroxyl groups, myricetin faces challenges in its poor water solubility and stability. These limitations, which affect its bioavailability and routes of administration, pose significant hurdles to developing myricetin as a pharmaceutical drug. Therefore, finding solutions to enhance the solubility of myricetin and improve its utilization will also be an important area of future research. The structural formula of myricetin is depicted in Figure 1.

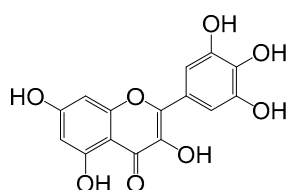


**Figure 1.** The structure of myricetin.

With the development of pesticide research, researchers have turned their attention to the direction of natural products in search of green and non-polluting pesticides [20]. Our group discovered myricetin as a promising compound in natural products. We studied myricetin due to its diverse biological activities and incorporated various active heterocyclic groups into its structure. As a result, we obtained compounds that demonstrated significant pesticide activities, including antibacterial and antiviral properties. For example, Jiang [21,22] synthesized compound **1** with an  $EC_{50}$  value of 1.58  $\mu\text{g}/\text{mL}$  for *Xanthomonas oryzae pv. Oryzae*, compound **2** with an  $EC_{50}$  value of 1.1  $\mu\text{g}/\text{mL}$  against *Xanthomonas axonopodis pv. Citri*. Chen [23] synthesized compound **3** with an  $EC_{50}$  value of 8.2  $\mu\text{g}/\text{mL}$  against *Xanthomonas oryzae pv. Oryzae*. Additionally, Peng [24] synthesized compound **4**, demonstrating curative and protective activities against TMV with  $EC_{50}$  values of 195.2 and 189.9  $\mu\text{g}/\text{mL}$ , respectively. These findings have laid the foundation for discovering more efficient and environmentally friendly botanical pesticides (Figure 2).

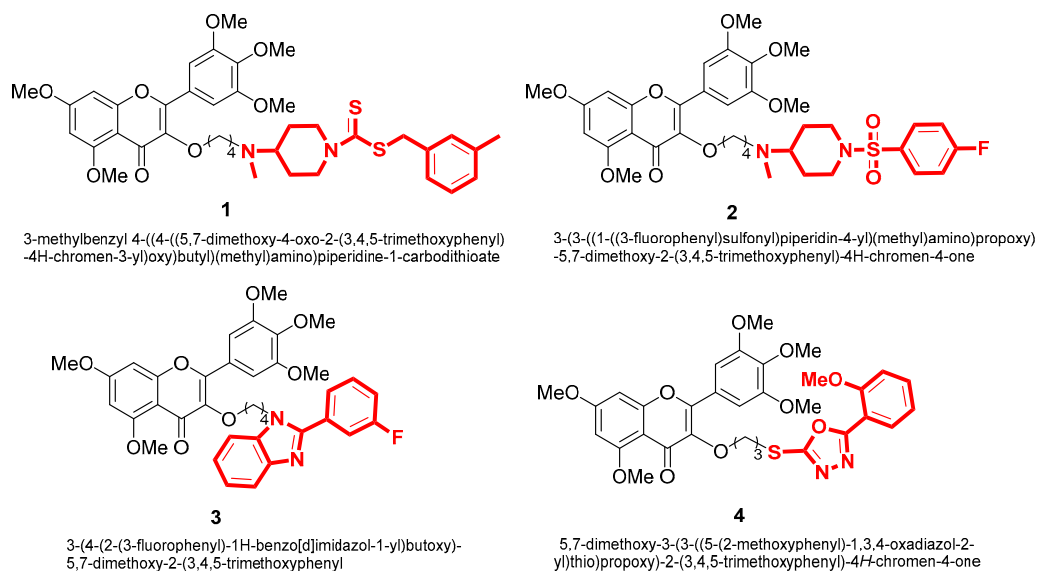


**Figure 2.** The structure of myricetin derivatives.

Amides contain a unique  $-\text{C}(=\text{O})-\text{NH}$  structure, where the oxygen can form hydrogen bonds with the ubiquinone binding site in succinate dehydrogenase (SDH), and the aromatic ring at the amino terminus binds to the Q site through hydrophobic and  $\pi$ - $\pi$  interaction, resulting in good biological activity. Amides find extensive applications in pesticides and pharmaceuticals [25]. Among the amide fungicides, succinate dehydrogenase

inhibitors (SDHI) are a class of fungicides with novel mechanisms of action, high efficiency and low toxicity, and significant development potential [26].

Pyrazoles are a class of nitrogen-containing five-membered heterocyclic compounds with a wide range of insecticidal [27,28], fungicidal [29,30] and herbicidal [31] activities. pyrazole-4-carbonyl compounds have exhibited good fungicidal activities, making them a hot structure in the research and development of agricultural fungicides [32]. Recent surveys indicated that among the 24 SDHI fungicides on the market, 12 are amide-based fungicides bearing pyrazole heterocycles in their acid components. This highlights the significant role of the pyrazole structure as a crucial pharmacophore in this class of fungicides. Notable commercialized examples of such fungicides include fluxapyroxad, pydiflumetofen, etc., all of which possess broad spectra and excellent antifungal activities (Figure 3) [33,34].

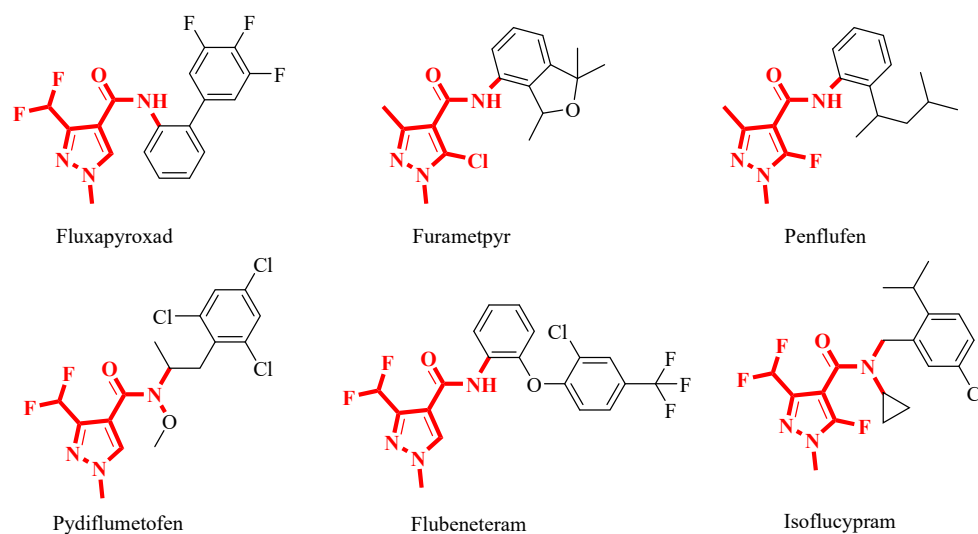


**Figure 3.** Commercialized SDHIs bearing a pyrazole-4-carboxamide fragment as agricultural fungicides.

Piperazine is an *N*-heterocyclic basic group that is easy to form multiple hydrogen bonds or ionic bonds. In medicinal chemistry, adjusting the physicochemical properties of compounds can enhance their water solubility, basicity, and biological activities [35]. Piperazine derivatives have attracted considerable interest in medicinal chemistry due to their therapeutic activities, including anti-mycobacterial, antibacterial, antiviral, antifungal, and antitumor effects [36–39]. In addition, piperazine derivatives have shown promising activities in combating phytopathogenic bacteria, making them valuable subjects for research [40].

Therefore, we introduced the pyrazole amide structure and the piperazine ring into the skeleton of myricetin to synthesize 19 derivatives, aiming to improve the biological activity of myricetin derivatives. The design strategy of the target compound is shown in Figure 4. In addition, their biological activities were evaluated, and the preliminary mechanism of compounds exhibiting excellent biological activity was explored.

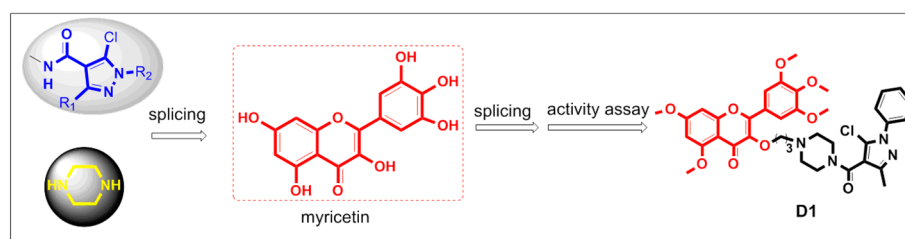
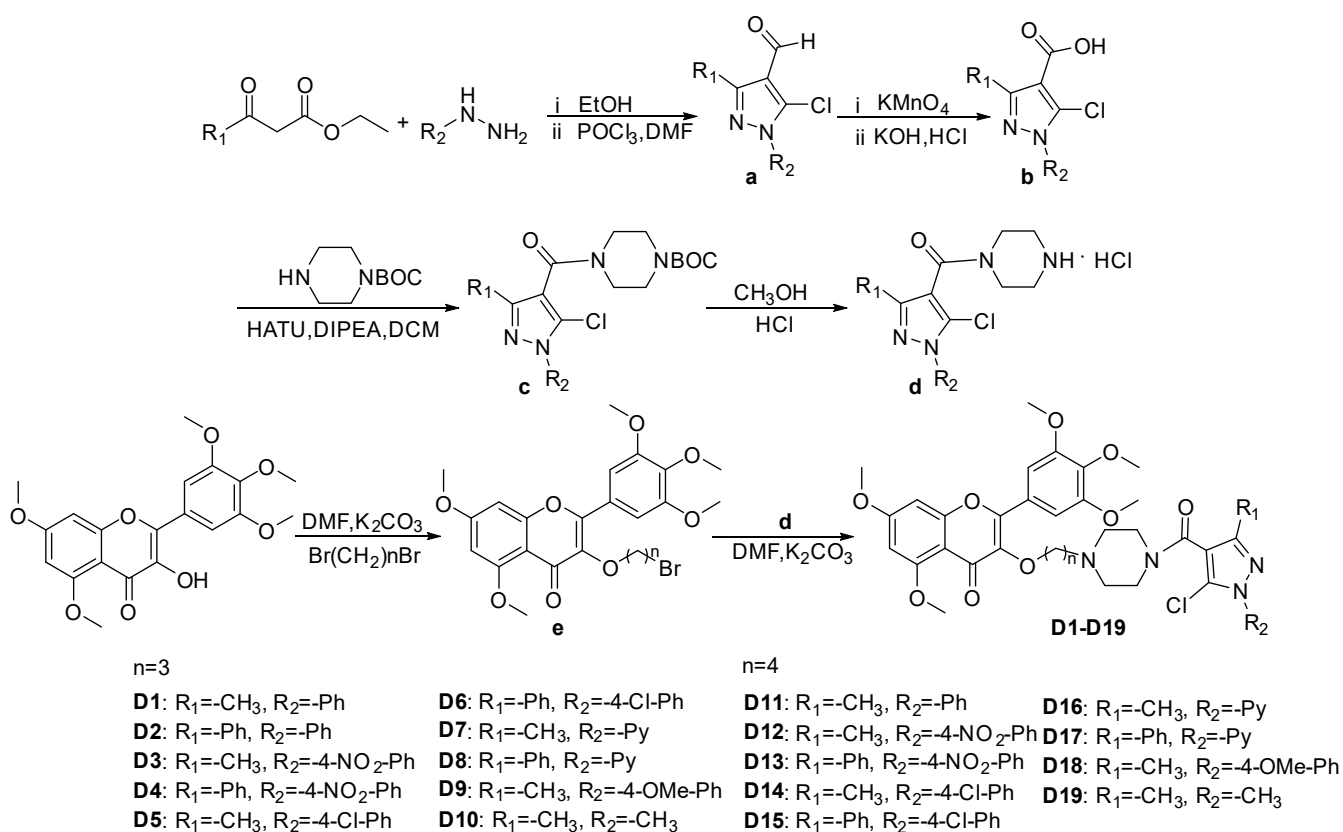


**Figure 4.** Design of the target compounds.

## 2. Result and Discussion

### 2.1. Chemistry

The synthetic route of title compounds **D1–D19** is illustrated in Scheme 1, based on the synthesis method outlined in reference [41–46]. The intermediate **a** was synthesized using substituted phenylhydrazine, ethyl acetoacetate or ethyl benzoylacetate, DMF (*N,N*-Dimethylformamide) and POCl<sub>3</sub> (phosphorus oxychloride). Subsequently, intermediate **a** reacted with potassium permanganate (KMnO<sub>4</sub>) under heating conditions, and intermediate **b** was obtained by adjusting pH. Further, Intermediate **b** was reacted with HATU (2-(7-Azabenzotriazol-1-yl)-*N,N,N',N'*-tetramethyluronium hexafluorophosphate), DIPEA (*N,N*-Diisopropylethylamine) and *N*-BOC-piperazine (tert-Butyl 1-piperazinecarboxylate) to synthesize intermediate **c** at room temperature. Intermediate **d** was obtained by adding methanol and HCl solution to the reaction bottle containing intermediate **c**. After adjusting the pH to neutral, DMF, K<sub>2</sub>CO<sub>3</sub> and intermediate **e** were added to synthesize the target compounds **D1–D19**, and their structures were confirmed by <sup>1</sup>H NMR, <sup>13</sup>C NMR, and HRMS data; the spectra information (Figures S1–S87) are provided in the Supporting Information.



**Scheme 1.** Schematic representation of the synthesis of target compounds **D1–D19**.

### 2.2. In Vitro Antibacterial Bioassay

The turbidimetric method was used to detect the inhibitory effects of **D1–D19** on the plant pathogenic bacteria *Psa*, *Xac* and *Xoo*. The results are shown in Table 1. Compound **D6** demonstrated an impressive 86.5% inhibition of *Xoo* at 100 µg/mL, superior to the commercial drugs thiodiazole-copper (85.8%) and bismethiazol (78.2%). At the concentration of 50 µg/mL, the inhibition of **D6** against *Xoo* was 76.7%, outperforming thiodiazole-copper (62.1%) and bismethiazol (57.4%). In addition, at 100 µg/mL, **D6** (49.7%), **D9** (39.5%) and **D13** (44.2%) showed higher inhibition against *Xac* than the control drugs, bismethiazol (35.6%) and myricetin (22.9%).

**Table 1.** In Vitro Antibacterial Activity of the Target Compounds at 100 µg/mL <sup>a</sup>.

Compd.	<sup>b</sup> <i>Psa</i>		<i>Xac</i>		<i>Xoo</i>	
	100 µg/mL	50 µg/mL	100 µg/mL	50 µg/mL	100 µg/mL	50 µg/mL
D1	37.0 ± 0.6	11.0 ± 0.2	14.7 ± 2.7	11.1 ± 2.9	14.9 ± 1.0	9.6 ± 2.1
D2	12.6 ± 0.2	9.0 ± 0.3	25.7 ± 0.3	16.8 ± 1.4	6.9 ± 0.4	1.6 ± 0.4
D3	31.6 ± 0.7	25.7 ± 0.5	32.7 ± 1.3	11.7 ± 5.3	5.7 ± 0.2	3.5 ± 1.6
D4	9.0 ± 1.6	7.2 ± 0.3	28.6 ± 2.1	20.0 ± 1.4	6.0 ± 1.3	1.4 ± 0.8
D5	42.2 ± 0.9	30.4 ± 0.9	9.4 ± 1.7	4.2 ± 1.5	16.8 ± 3.2	9.2 ± 1.8
D6	10.8 ± 0.7	8.5 ± 0.7	49.7 ± 1.4	31.3 ± 0.9	86.5 ± 1.8	76.7 ± 0.7
D7	10.2 ± 0.2	9.42 ± 0.3	23.4 ± 0.9	11.1 ± 0.9	21.5 ± 1.1	16.4 ± 1.5
D8	10.7 ± 1.1	8.7 ± 0.6	27.6 ± 0.2	17.2 ± 0.3	19.6 ± 0.9	15.3 ± 1.9
D9	38.8 ± 0.2	22.8 ± 0.4	39.5 ± 2.2	20.8 ± 3.5	4.3 ± 0.2	3.6 ± 0.2
D10	18.6 ± 0.4	12.8 ± 0.5	8.0 ± 2.7	7.0 ± 1.6	28.3 ± 1.9	19.2 ± 1.0
D11	16.0 ± 0.1	11.6 ± 0.5	12.9 ± 0.7	10.8 ± 0.3	14.4 ± 1.1	10.6 ± 0.2
D12	13.0 ± 2.0	12.1 ± 0.4	19.0 ± 0.4	17.8 ± 1.1	15.3 ± 0.0	7.7 ± 0.1
D13	12.5 ± 0.9	11.6 ± 0.3	44.2 ± 0.6	24.3 ± 0.3	12.1 ± 0.6	9.5 ± 0.7
D14	8.4 ± 0.4	8.0 ± 0.54	30.4 ± 3.1	18.5 ± 2.4	14.2 ± 1.1	11.8 ± 1.7
D15	14.9 ± 0.5	9.4 ± 0.3	19.5 ± 2.8	11.8 ± 3.0	15.2 ± 0.5	9.3 ± 1.5
D16	9.7 ± 0.6	9.1 ± 0.6	34.7 ± 0.7	28.0 ± 2.1	15.6 ± 2.5	7.0 ± 5.0
D17	16.7 ± 0.9	11.8 ± 0.8	9.9 ± 2.4	8.0 ± 0.8	12.1 ± 3.2	5.1 ± 3.9
D18	12.4 ± 0.3	11.5 ± 0.2	31.0 ± 0.5	29.6 ± 1.4	16.4 ± 3.4	11.2 ± 1.4
D19	18.0 ± 0.9	13.4 ± 0.63	20.6 ± 0.9	16.5 ± 0.7	12.0 ± 1.1	7.8 ± 0.9
TC <sup>c</sup>	65.8 ± 0.3	20.0 ± 0.2	80.1 ± 3.4	53.0 ± 0.3	85.8 ± 0.9	62.1 ± 0.7
BT <sup>c</sup>	26.5 ± 0.2	24.8 ± 0.5	35.6 ± 4.7	27.4 ± 4.0	78.2 ± 0.6	57.4 ± 1.0
Myr. <sup>c</sup>	18.5 ± 0.3	11.5 ± 0.2	22.9 ± 1.3	20.3 ± 1.9	32.0 ± 4.5	15.1 ± 0.3

<sup>a</sup> Values are mean ± SD of three replicates. <sup>b</sup> *Xac* (*Xanthomonas axonopodis* pv. *Citri*), *Psa* (*Pseudomonas syringae* pv. *Actinidiae*) and *Xoo* (*Xanthomonas oryzae* pv. *Oryzae*); <sup>c</sup> BT (bismethiazol), TC (thiodiazole copper) and Myr. (myricetin).

Table 1 data shows that when  $n = 3$ ,  $R_1 = -CH_3$ , the series of compounds have better inhibitory activity against *Psa*, such as **D1**, **D3**, **D5**, **D9**. In addition, the inhibitory activity of **D5** (42.2%) against *Psa* was better than that of **D1** (37%), **D3** (31.6%) and **D9** (38.8%). At the same time, when  $n = 3$ ,  $R_1 = -Ph$ , the inhibitory activity of compound **D6** against *Xac* (49.7%) and *Xoo* (86.5%) was higher. In summary, it is shown that when  $n = 3$ , the substituent  $-Cl$  on the benzene ring can improve the antibacterial activity of the compound. Subsequently, the  $EC_{50}$  values of **D6**, which had excellent inhibitory activity against *Xoo*, were further evaluated, and the results are presented in Table 2. The results revealed that **D6** had an  $EC_{50}$  value of 18.8 µg/mL, which was significantly higher than that of the commercial agents thiodiazole-copper (52.9 µg/mL) and bismethiazol (69.1 µg/mL).

**Table 2.** The  $EC_{50}$  values of Compound **D6** against *Xoo* <sup>a</sup>.

Compound	$EC_{50}$ (µg/mL)	Toxic Regression Equation	$r^2$
D6	18.8 ± 1.2	$y = 1.4509x + 2.7846$	0.9518
BT	69.1 ± 2.4	$y = 2.0188x + 1.6209$	0.9414
TC	52.9 ± 1.5	$y = 0.9657x + 2.3405$	0.9589

<sup>a</sup> Values are mean ± SD of three replicates.

### 2.3. In Vitro Antifungal Bioassay

The inhibitory activities of the compounds against ten plant pathogenic fungi were determined at 100 µg/mL using azoxystrobin as a control agent. The results are presented in Table 3. The inhibitory effects of **D1** (82.3%), **D2** (72.1%), **D3** (80.5%) and **D9** (81.4%) against *Phomopsis* sp. were better than that of commercial drug azoxystrobin (59.5%). Similarly, **D1** (67.9%) displayed a comparable inhibitory effect to the azoxystrobin (72.8%) against *B. dothidea*. Furthermore, **D1** (37.9%) showed a similar inhibitory effect azoxystrobin (45.1%) against *C. gloeosporioides*. And it also had inhibitory activities against *P. capsici* and *N. dimidiatum*, with inhibition rates of 50.4% and 67.4%, respectively. In summary,

compound **D1** showed inhibitory activity against various fungi. To further investigate its mechanism of action, fluopyram was selected as the control agent and *Phomopsis* sp. as the test strain. Its biological activity was measured, and the results showed that the inhibitory activity of **D1** (82.3%) against *Phomopsis* sp. was better than that of fluopyram (48.2%).

**Table 3.** In Vitro Antifungal Activities of the Title Compounds **D1–D19** at 100 µg/mL<sup>a</sup>.

Compd.	<sup>b</sup> Ps	<sup>b</sup> Pc <sup>1</sup>	<sup>b</sup> Bd	<sup>b</sup> Bc	<sup>b</sup> Cg	<sup>b</sup> Fg	<sup>b</sup> Fd	<sup>b</sup> Ss	<sup>b</sup> Pc	<sup>b</sup> Nd
<b>D1</b>	82.3 ± 0.0	81.2 ± 1.2	67.9 ± 1.6	66.1 ± 0.0	37.9 ± 2.6	24.8 ± 2.9	31.9 ± 1.6	25.6 ± 3.0	50.4 ± 1.0	67.4 ± 1.0
<b>D2</b>	72.1 ± 1.6	45.2 ± 1.7	41.5 ± 2.4	59.0 ± 2.1	15.6 ± 2.3	18.4 ± 1.2	-	46.8 ± 2.0	43.0 ± 1.0	22.2 ± 2.8
<b>D3</b>	80.5 ± 1.2	37.8 ± 1.1	32.9 ± 3.5	52.2 ± 1.4	19.9 ± 2.4	20.4 ± 7.8	11.3 ± 2.2	59.8 ± 1.2	28.5 ± 1.5	24.4 ± 2.5
<b>D4</b>	-	33.0 ± 2.7	-	36.2 ± 2.1	16.8 ± 1.8	-	-	15.6 ± 3.1	26.3 ± 0.8	-
<b>D5</b>	64.3 ± 2.2	76.2 ± 1.2	65.7 ± 2.1	64.9 ± 1.2	30.1 ± 0.9	16.0 ± 6.1	60.1 ± 1.8	53.2 ± 1.6	46.7 ± 0.0	57.8 ± 2.1
<b>D6</b>	55.8 ± 3.5	50.6 ± 1.2	23.9 ± 2.2	62.2 ± 2.3	17.6 ± 1.6	15.5 ± 1.2	10.5 ± 1.4	33.8 ± 1.7	31.1 ± 1.3	18.9 ± 2.1
<b>D7</b>	11.2 ± 1.0	69.0 ± 1.2	22.6 ± 2.3	35.5 ± 2.9	20.7 ± 6.4	23.4 ± 3.4	-	19.8 ± 1.8	36.3 ± 1.6	-
<b>D8</b>	-	22.8 ± 2.3	-	39.4 ± 2.0	18.4 ± 0.9	15.5 ± 1.8	-	14.4 ± 2.2	24.4 ± 1.8	-
<b>D9</b>	81.4 ± 1.3	77.0 ± 0.9	57.8 ± 1.9	74.5 ± 1.8	27.3 ± 1.3	29.3 ± 2.2	35.9 ± 1.2	54.8 ± 2.6	44.1 ± 0.8	65.2 ± 1.6
<b>D10</b>	-	68.2 ± 1.2	19.6 ± 3.9	28.9 ± 3.7	12.9 ± 4.5	20.0 ± 2.9	12.1 ± 1.1	26.8 ± 2.8	24.8 ± 1.9	17.8 ± 2.1
<b>D11</b>	20.3 ± 2.9	27.7 ± 1.2	45.5 ± 3.9	28.5 ± 1.8	16.0 ± 3.8	13.6 ± 4.5	-	15.8 ± 3.0	24.4 ± 1.3	-
<b>D12</b>	17.7 ± 3.0	45.2 ± 1.7	40.0 ± 3.5	41.0 ± 2.5	17.2 ± 4.3	10.4 ± 5.0	-	33.8 ± 1.7	21.5 ± 1.0	-
<b>D13</b>	11.2 ± 1.0	36.4 ± 2.3	40.4 ± 3.9	41.4 ± 3.5	14.8 ± 1.7	23.4 ± 2.3	-	38.0 ± 2.8	23.3 ± 2.1	11.1 ± 0.0
<b>D14</b>	-	39.0 ± 1.2	10.7 ± 1.8	37.4 ± 1.9	10.9 ± 1.3	30.1 ± 1.7	-	40.9 ± 2.3	20.4 ± 1.5	21.9 ± 0.8
<b>D15</b>	15.1 ± 2.2	47.8 ± 2.0	32.9 ± 3.5	63.8 ± 0.9	-	19.2 ± 1.7	-	46.8 ± 1.4	29.3 ± 0.8	10.0 ± 1.1
<b>D16</b>	-	72.8 ± 0.9	-	40.2 ± 1.7	-	27.6 ± 2.6	10.9 ± 1.6	41.8 ± 1.4	28.2 ± 1.0	-
<b>D17</b>	25.1 ± 2.4	59.0 ± 1.2	-	35.5 ± 1.9	17.6 ± 6.7	21.8 ± 4.8	-	27.4 ± 2.7	35.6 ± 0.0	23.7 ± 1.6
<b>D18</b>	13.5 ± 1.6	56.1 ± 1.9	-	41.8 ± 1.0	12.5 ± 1.1	24.3 ± 3.0	-	46.4 ± 1.7	28.2 ± 1.6	-
<b>D19</b>	14.7 ± 1.7	76.2 ± 1.2	-	21.9 ± 1.4	13.3 ± 1.3	11.2 ± 5.9	-	25.2 ± 2.2	28.2 ± 1.0	19.6 ± 1.5
Az <sup>c</sup>	59.5 ± 0.7	58.2 ± 3.4	72.8 ± 1.5	90.7 ± 1.5	45.1 ± 0.9	44.8 ± 1.4	55.8 ± 1.5	74.4 ± 1.2	91.1 ± 2.8	91.1 ± 2.8
Myr. <sup>c</sup>	22.8 ± 3.4	46.4 ± 2.2	-	22.8 ± 1.8	-	-	-	25.2 ± 1.1	18.5 ± 2.1	-
Fl <sup>c</sup>	48.2 ± 1.4	-	-	-	-	-	-	-	-	-

<sup>a</sup> Values are mean ± SD of three replicates. <sup>b</sup> Ps, *Phomopsis* sp.; Pc<sup>1</sup>, *P. capsici*; Bd, *B. dothidea*; Bc, *B. cinerea*; Cg, *C. gloeosporioides*; Cc, *C. capsici*; Fg, *F. graminearum*; Fd, *F. dimerum*; Ss, *S. sclerotiorum*; Rs, *R. solani*; Pc, *P. cucumerina*; Nd, *N. dimidiatum*. <sup>c</sup> Azoxystrobin (Az), Fluopyram (Fl) and Myricetin (Myr.) were used as the control agents.

Table 3 demonstrated that introducing pyrazole piperazine amide can enhance the antifungal activity of myricetin. In this study, we investigated the association of the pyrazole ring with the parent structure of myricetin and the structures of the substituent group on the pyrazole ring of the compound and analyzed their structure-activity relationships. First, the inhibition activity of the compounds was generally higher when n = 3 (n = number of carbons) than n = 4, demonstrating that the inhibition activity of the target compounds generally decreased with the growth of the carbon chain. Also, we found that the inhibition activity of compounds with R<sub>1</sub> = -CH<sub>3</sub> was generally superior to compounds with R<sub>1</sub> = -Ph (phenyl), such as **D1** > **D2**, **D3** > **D4**, **D5** > **D6**, **D7** > **D8**, **D9** > **D10**. In addition, when R<sub>2</sub> = -Ph, -4-NO<sub>2</sub>-Ph, -4-Cl-Ph and -4-OMe-Ph, it has inhibitory activity against various fungi, such as **D1**, **D3**, **D5**, and **D9**. In addition, from compounds **D16** (72.8%) and **D19** (76.2%), it can be speculated that the inhibition activity may depend on the exposed heterocyclic structure when the heterocyclic group is far away from the parent structure of myricetin. Based on the in vitro antifungal experiment demonstrated that the introduction of the pyrazole piperazine amide group into the myricetin parent structure could generally improve its biological activity. And when n = 3 and R<sub>1</sub> = -CH<sub>3</sub> can effectively improve the antibacterial activity of the compound. To verify the antifungal activity of these compounds more accurately and visually, we determined the half-maximal effective concentration values (EC<sub>50</sub>) of the compounds with higher inhibition than the control agent at 100 µg/mL, and the results are shown in Table 4. The results showed that inhibitory activities of **D1** (16.9 µg/mL), **D2** (19.7 µg/mL) and **D9** (20.3 µg/mL) against *Phomopsis* sp. were superior to control drugs azoxystrobin (50.7 µg/mL) and fluopyram (71.8 µg/mL). In addition, the EC<sub>50</sub> values of **D1**, **D5**, **D9**, **D10** and **D16** showed between 11.3 and 30.2 µg/mL against *P. capsici*, which were higher than azoxystrobin (35.1 µg/mL) and **D16** (11.3 µg/mL) showed the best performance.

**Table 4.** EC<sub>50</sub> values of Several Target Compounds <sup>a</sup>.

Compound	Phytopathogen	EC <sub>50</sub> (µg/mL)	Toxic Regression Equation	r <sup>2</sup>
D1	<i>Ps</i>	16.9	y = 1.1324x + 3.6102	0.9642
D2	<i>Ps</i>	19.7	y = 0.5472x + 4.2918	0.9355
D9	<i>Ps</i>	20.3	y = 0.7801x + 3.9800	0.9744
Fluopyram	<i>Ps</i>	71.8	y = 0.5860x + 3.9123	0.9086
Azoxystrobin	<i>Ps</i>	50.7	y = 0.7262x + 3.7617	0.9935
D1	<i>Pc</i> <sup>1</sup>	29.6	y = 0.7650x + 3.8744	0.9893
D5	<i>Pc</i> <sup>1</sup>	18.5	y = 0.3051x + 4.6137	0.9319
D9	<i>Pc</i> <sup>1</sup>	21.7	y = 0.4435x + 4.4074	0.9535
D16	<i>Pc</i> <sup>1</sup>	11.3	y = 0.3550x + 4.6266	0.9241
Azoxystrobin	<i>Pc</i> <sup>1</sup>	35.1	y = 0.4919x + 4.2402	0.9717

<sup>a</sup> The experiments were repeated three times.

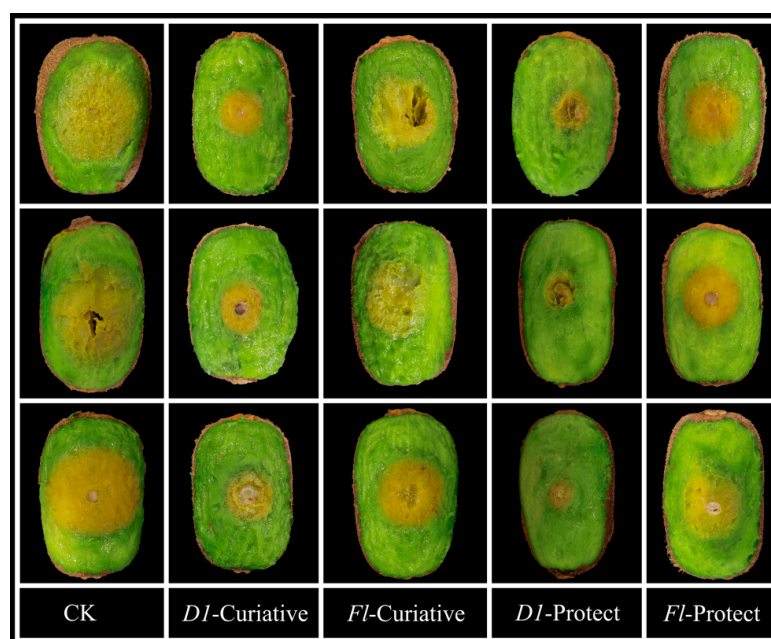
#### 2.4. Inhibitory Effect of D1 on *Phomopsis* sp. In Vitro

Fresh, uniformly sized kiwifruits with no surface damage were selected for experimental studies using the agricultural fungicide fluopyram as a controlled drug. D1 showed better fungicidal activity against *Phomopsis* sp. than the control drug. Therefore, D1 was chosen to perform the test to verify its in vitro curative and protective activities against kiwifruit inoculated with *Phomopsis* sp. As shown in Table 5 and Figure 5, the treatment of kiwifruits with D1 displayed 74.9% protective and 60.6% curative effects, superior to the protective and curative effects of fluopyram (41.4 and 32.5%, respectively). Based on these facts, we can conclude that D1 has good antifungal activity in vitro.

**Table 5.** Curative and Protective Activities of D1 Against *Phomopsis* sp. In Vitro.

Treatment	Concentration (200 µg/mL)	Curative Effect		Protective Effect	
		Lesion Length <sup>a</sup> (mm ± SD)	Controlling Efficacy (%)	Lesion Length <sup>a</sup> (mm ± SD)	Controlling Efficacy (%)
D1		18.3 ± 1.5	60.6 ± 3.9	13.5 ± 1.5	74.9 ± 3.9
fluopyram <sup>b</sup>		27.8 ± 1.7	32.5 ± 4.4	24.8 ± 1.2	41.4 ± 3.0
control		38.8 ± 2.5			

<sup>a</sup> Values are mean ± SD of three replicates. <sup>b</sup> The commercial antifungal agent.

**Figure 5.** Protective Activity of D1 and Fluopyram Against *Phomopsis* sp. on Kiwifruit.

### 2.5. Light Microscope Observation of Compound **D1** on the Hyphae Morphology

After **D1** (12.5  $\mu\text{g}/\text{mL}$ ) treatment, *Phomopsis* sp. hyphae were observed under a microscope ( $100 \times 1.25$ ), as depicted as in Figure 6. Specifically, compared to the blank control group (0.5% DMSO), the growth of *Phomopsis* sp. Mycelia were inhibited upon being treated with **D1**. Additionally, increased branching, production of short hyphae and uneven thickness distribution were observed.

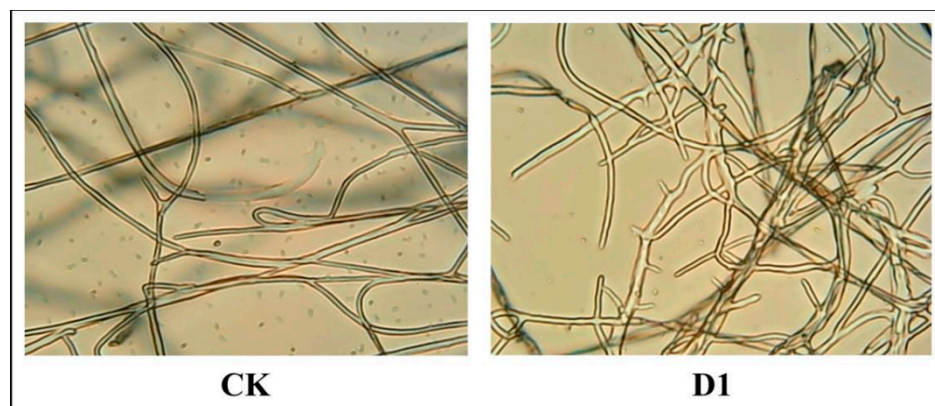


**Figure 6.** **D1** (right) treatment group and untreated group (CK, left).

### 2.6. Inhibitory Effect of **D1** on SDH In Vitro

Since the structure of this series of compounds is similar to that of succinate dehydrogenase inhibitors, to explore whether SDH is the action site of compound **D1**, the following experiments were carried out. The effects of the target compound **D1** and fluopyram on SDH activity were compared under the same conditions. The experiments involved treating the *Phomopsis* sp. with different concentrations of the drugs and incubating them at a constant temperature of 28  $^{\circ}\text{C}$  for 24 h. The results are shown in Figure 7. Compared with the control drug fluopyram, **D1** had a greater effect on SDH activity and could effectively inhibit SDH activity in a concentration-dependent manner. This result indicates that SDH may be one of the action sites of compound **D1**.

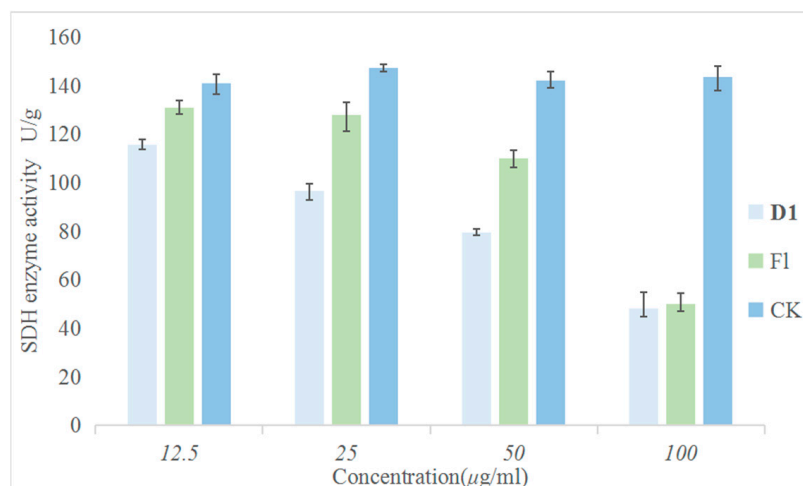


**Figure 7.** Inhibitory Effect of Different Concentrations of **D1** and Fluopyram on SDH.

### 2.7. Molecular Docking of **D1** to SDH

The molecular docking results are shown in Figure 8. In this figure, the compounds **D1** and fluopyram are embedded in similar binding modes into the active protein pocket of SDH. These conformations interact with the surrounding amino acid residues via carbon-hydrogen, conventional hydrogen, Pi-alkyl, alkyl, and Pi-sigma. **D1** formed three carbon-

hydrogen bonds with THR79 (3.30 Å), SER54 (3.04 Å) and LEU51 (4.50 Å) active sites of SDH, respectively, and fluopyram formed a conventional hydrogen bond with GLY71 (2.07 Å). **D1** formed four Pi-alkyl hydrophobic interactions and alkyl interactions with ILE55 (4.83 Å), LEU72 (4.20 Å), LEU75 (4.86 Å) and VAL54 (4.90 Å). Fluopyram formed five alkyl and Pi-alkyl interactions with LEU75 (4.50, 5.00 and 5.00 Å), ILE78 (4.27 Å) and LEU58 (4.11 Å). In addition, **D1** forms four Pi-sigma interactions with multiple amino acid residues of SDH, such as LEU51 (3.92 Å), LEU58 (3.28 Å) and ILE78 (3.58 and 3.61 Å). Fluopyram forms a Pi-sigma interaction with LEU58 (3.65 Å) and a halogen interaction with LEU75 (3.34 Å). In summary, **D1** forms multiple interactions with the amino acid residues of SDH, making it tightly bound to SDH. At the same time, the docking fraction of **D1** was  $-5.50$ , which was better than that of fluopyram at  $-4.55$ . It is further proved that SDH may be one of the action sites of **D1**. It is proved that **D1** may affect the tricarboxylic acid cycle by combining with SDH, leading to the final death of fungi.

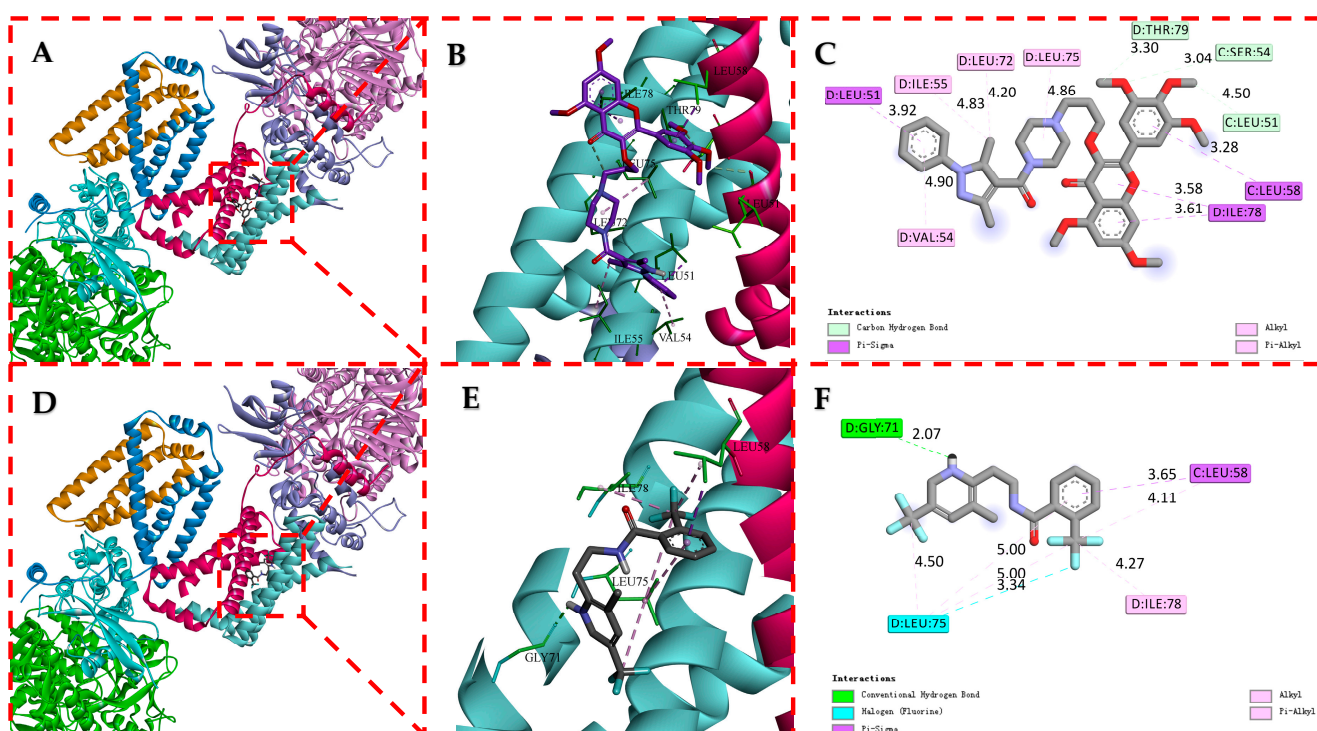


**Figure 8.** Molecular Docking Modes of **D1** (A–C) and Fluopyram (D–F) with SDH.

### 2.8. Effect of **D1** on the Cytoplasmic Leakage of *Phomopsis sp.*

To explore other possible modes of action of compound **D1**, the damage degree of mycelium after drug action was determined. Among them, the malondialdehyde (MDA) content can indirectly reflect the degree of tissue peroxidation damage in the membrane of mycelium, and the higher the content, the more serious the damage to the cell membrane. The results are shown in Figure 9. The content of MDA in *Phomopsis sp.* mycelium treated with different concentrations of **D1** (0, 12.5, 25, 50 and 100  $\mu\text{g}/\text{mL}$ ) gradually increased with increasing concentration and was better than the control group. The results show that **D1** can cause damage to the cell membrane, and the degree of damage increases with the increase in concentration. It indicates that compound **D1** may also damage the cell membrane structure by destroying the permeability of the cell membrane so that the drug penetrates the bacteria and binds to certain enzymes, affecting the enzyme activity and thereby achieving the antibacterial effect.

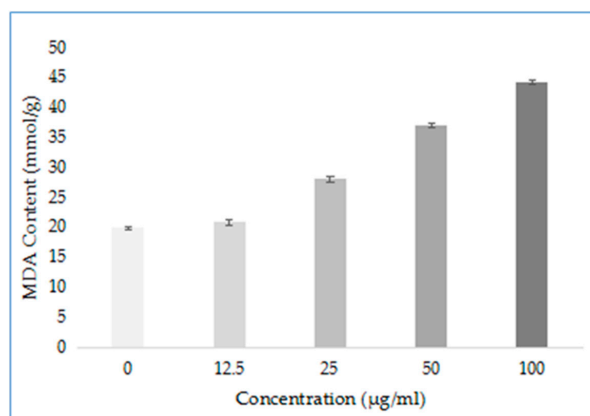


**Figure 9.** MDA Content of *Phomopsis* sp. after Treatment with D1.

### 2.9. Effect of Compound D16 on Mycelial Morphology of *P. capsici*

Mycelium of *P. capsici* was treated with 100 µg/mL DMSO (A) and D16 (B). As shown in Figure 10, the results showed that the mycelium had a smooth surface, great growth, and intact structure after DMSO treatment. However, after D16 treatment, it experienced shrinkage and folding, with shortened and prominent branches. These changes altered the morphology of the mycelium and significantly inhibited its growth.

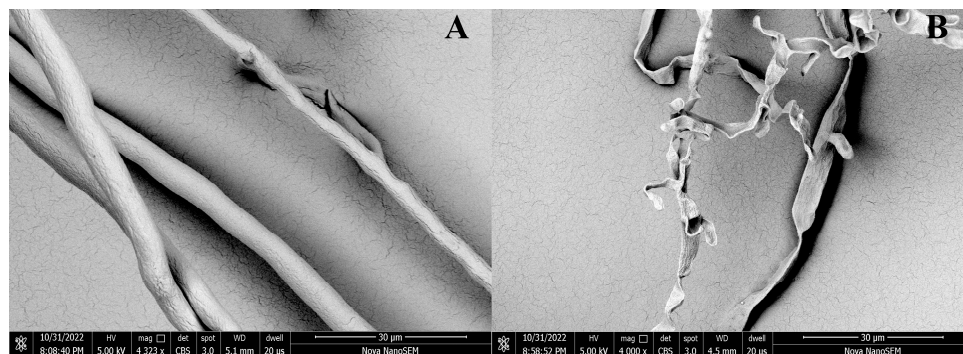


**Figure 10.** SEM Images of the Hyphae of *P. capsici* after Treatment with D16 (B) and CK (A).

## 3. Materials and Methods

### 3.1. Instruments and Chemicals

All reagents were purchased from Shanghai Titan Chemical Co., Ltd. (Shanghai, China) and Ptsrti, Ltd. (Chongqing, China). Enzyme activity kits were purchased from Beijing Solarbio Science & Technology Co., Ltd. (Beijing, China). The melting point data were measured by the X-4B melting point instrument (Shanghai INESA Co., Ltd., Shanghai, China) without correction. Spectral data was measured by a 400 NMR spectrometer with dimethylsulfoxide- $d_6$  as the solvent (Bruker, Karlsruhe, Germany). HRMS data were recorded using a hybrid quadrupole mass spectrometer (Thermo Scientific, Waltham, MA, USA). Image data was obtained on the Olympus CX21FS1 microscope (Tokyo, Japan). Scanning electron microscopy (SEM), data were obtained on FEI Nova Nano 450 (Hillsboro, OR, USA). Thin layer chromatography (TLC) analysis was adopted by a WFH-203B ultraviolet analyzer (Shanghai Jingke Industrial Co., Ltd., Shanghai, China).

#### 3.1.1. Synthesis of Intermediate a

Substituted phenylhydrazine (10.4 mmol) and 10 mL anhydrous ethanol were stirred and heated in a 50 mL reaction flask to about 50 °C. Ethyl acetoacetate or ethyl benzoylacetate (10.4 mmol) was then added dropwise. The reaction was refluxed for 5 h to complete, and the solvent was evaporated under reduced pressure to obtain pyrazolone. Take another 100 mL reaction flask, add DMF (29.63 mmol) was added, ice bath to 0 °C,  $POCl_3$

(70.26 mmol) was slowly added and stirred for 20 min. The above pyrazolone compound was then added slowly. The mixture warmed up to 85 °C and refluxed for 5 h. The progress of the reaction was monitored using TLC (Ethyl acetate: Petroleum ether = 2:1). After cooling to room temperature. The reaction mixture was slowly poured into ice water with constant stirring to accelerate heat dissipation. It was then cooled and left to stand, and intermediate **a** was obtained by filtration, washing, and drying, with a yield of 32–92%.

### 3.1.2. Synthesis of Intermediate **b**

The intermediate **a** (7.07 mmol) was taken in a 250 mL reaction bottle, and then  $\text{KMnO}_4$  solution (9.2 mmol) was added. The reaction was heated to 80 °C and refluxed for about 8 h. TLC (ethyl acetate: petroleum ether = 2:1) was monitored until the intermediate **a** was completely consumed. After the reaction was cooled to room temperature, the pH was adjusted to alkaline with freshly prepared 10% KOH solution. The insoluble material was removed through filtration, and the resulting transparent filtrate was collected. The pH of the filtrate was then adjusted to acidic by using 10% HCl. The precipitated solid was filtered and dried to obtain intermediate **b**. The yield was 36–91%.

### 3.1.3. Synthesis of Intermediate **c**

The intermediate **b** (5.52 mmol) was taken in a 100 mL round bottom flask, and mixed with 20 mL DCM (dichloromethane), HATU (6.63 mmol), and DIPEA (8.29 mmol), stirred for 30–45 min at room temperature. Subsequently, N-BOC-piperazine (6.08 mmol) was added and reacted overnight. Then extracted with DCM, the lower extract was collected, the solvent was removed by distillation under reduced pressure, and intermediate **c** was purified by column chromatography with a 14–86% yield.

### 3.1.4. Synthesis of Intermediate **d**

Weigh intermediate **c** (3.61 mmol) in a 100 mL reaction flask. Add 20 mL of methanol to the flask, slowly add HCl (18 mmol) and react at room temperature until complete. Then, distil under reduced pressure several times to remove HCl and solvent to obtain intermediate **d**. The intermediate **d** was adjusted to neutral pH and entered the next reaction directly.

### 3.1.5. Synthesis of Intermediate **e**

2.5 g (6.4 mmol) of methylated myricetin and 2.67 g (19.3 mmol) of anhydrous  $\text{K}_2\text{CO}_3$  were taken in a 100 mL reaction flask. 50 mL of DMF was added and stirred for about 30 min at room temperature. Subsequently, 1.96 mL (19.3 mmol) of 1,3-dibromo butane was added dropwise and stirred for 10 h at room temperature. Then the reaction mixture was dispersed in 100 mL of distilled water, leading to the precipitate of a white solid. The solid was then filtered, dried, and poured into a mixed solvent reaction vial containing 60 mL (petroleum ether: ethyl acetate = 1:3, V/V). The mixture was stirred for 4–5 h at room temperature, and then filtered and dried to obtain intermediate **e**. The yield was 72%.

### 3.1.6. Synthesis of Intermediate **D1–D19**

DMF (20 mL) and anhydrous  $\text{K}_2\text{CO}_3$  (17.68 mmol) were added to the reaction flask in Section 3.1.4 and then stirred at room temperature for about 45 min. The intermediate **e** (2.95 mmol) was added. And the reaction was carried out at 100 °C for about 5–7 h. After the complete reaction, the reaction system was slowly dispersed in 100 mL of ice water and extracted with DCM (3 × 20 mL). The crude product was obtained by distillation under reduced pressure to remove the solvent and finally purified by column chromatography (ethyl acetate:methanol = 80:1–60:1, V/V) to obtain the target compounds **D1–D19**, in 4–64% yield.

## 3.2. Antibacterial Activity Bioassay In Vitro

According to the literature [47], the in vitro antibacterial activity of compounds **D1–D19** against three plant pathogenic bacteria was determined by the turbidimetric method.

*Xanthomonas oryzae* pv. *Oryzae* (Xoo), *Xanthomonas axonopodis* pv. *Citri* (Xac) and *Pseudomonas syringae* pv. *Actinidiae* (Psa) were used as test strains. The prepared NB (Nutrient Broth) medium was sterilized at 121 °C for 20 min. Then the compounds to be tested were dissolved in DMSO and mixed with NB medium to obtain a final concentration of 100 µg/mL. The mixture was added to a 96-well plate, followed by the addition of the prepared bacterial culture (DMSO mixture containing bacteria was used as the negative control, and thiramycin and chlorothalonil were used as the positive control). Another 96-well plate (NB medium with drug and no bacteria) was used as a blank control. The two well plates were sealed and incubated in a constant temperature shaker until the OD<sub>595 nm</sub> value of the negative control was 0.6–0.7. The OD<sub>595 nm</sub> values of all bacterial cultures were measured. Triplicates were set for each treatment, and each experiment was repeated three times. The formula was calculated as follows:

$$I(\%) = (C - T)/C \times 100\%$$

I—inhibition rate

C—OD<sub>595 nm</sub> (control medium after correction)

T—OD<sub>595 nm</sub> (drug-containing medium after correction)

According to the above method, the inhibition rates of 100, 50, 25, 12.5, and 6.25 µg/mL were tested. The inhibition rate was converted into probability value (y), and the concentration of the drug solution was converted into logarithmic value (x). The data were processed by Excel software (2021) to obtain the virulence regression equation ( $y = ax + b$ ) and correlation coefficient (R) to calculate the half maximal effective concentration (EC<sub>50</sub>) of the excellent compound against the pathogen.

### 3.3. Scanning Electron Microscope (SEM) Observation

To further investigate the mechanism of action of these compounds, scanning electron microscopy experiments were carried out with reference to the literature [48,49]. The mycelium treated with **D16** (*P. capsici*) was washed with 0.1 mol/L phosphate buffer (pH = 7.2), fixed in 2.5% glutaraldehyde overnight (4 °C), dehydrated with gradient ethanol, and finally fixed in tert-butanol for 10 min, freeze-dried for about 3 h. The Specimens have been loaded on SEM stubs, sputter-coated with gold, and observed under SEM.

### 3.4. Antifungal Activity Bioassay In Vitro

According to the method reported in the literature, the antifungal activities of the compounds were evaluated with the mycelial growth rate method [50–52]. *Phytophthora capsici* (Pc<sup>1</sup>), *Phomopsis* sp. (Ps), *Botryosphaeria dothidea* (Bd), *Botrytis cinerea* (Bc), *Fusarium graminearum* (Fg), *Fusarium dimerum* (Fd), *Colletotrichum gloeosporioides* (Cg), *Plectosphaerella cucumerina* (Pc), *Sclerotinia sclerotiorum* (Ss) and *Neoscytalidium dimidiatum* (Nd) were used as test strains. Firstly, the prepared PDA (Potato Dextrose Agar) medium was sterilized at 121 °C for 20 min. DMSO (0.5%) was the blank control, and azoxystrobin and fluopyram as a positive control. Then the compound to be tested was dissolved in DMSO to make a solution. The solution was then added to the PDA medium to a final concentration of 100 µg/mL. The mixture was thoroughly shaken well and poured into a sterile petri dish. A 5-mm diameter sterile punch was used to punch holes at the edge of the newly activated strains. Subsequently, the blocks were picked with a sterile needle and placed in the center of the drug-containing medium in the above spare petri dishes. Triplicates were set for each treatment, and each experiment was repeated three times. When the mycelium of the blank control group grew until it spread all over the petri dish, the diameter of mycelium growth was measured by the crossover method. The calculation formula was as follows:

$$I(\%) = (C - T)/(C - 5) \times 100\%.$$

“I”—inhibition rate; “C”—blank control; “T”—drug treatment.

### 3.5. In Vitro Antifungal Experiment of D1 on Kiwifruit

In vitro, bioactivity assay tests were conducted according to the references [53,54]. The in vitro control effect of compound D1 against *Phomopsis* sp. was determined using the kiwifruit variety "Miliang No 1" as experimental material and the fluopyram as a control drug. To study the curative and protective effects of D1 on kiwifruit, fresh, uniformly sized kiwifruit fruits with undamaged surfaces were selected for the experimental study, disinfected by immersion in 1% NaClO solution and washed with sterile water. Then the surface water was wiped with filter paper. To evaluate the protective activity, the fruit surface was punched holes (5-mm), and then the prepared D1 (200 µg/mL) was sprayed uniformly on the surface of kiwifruit fruit, with aqueous DMSO (1%) solution as a blank control. And 5-mm agar blocks containing mycelium were placed on the fruit perforations after 24 h in the incubator. To evaluate the curative activity, agar blocks containing mycelium were inoculated at the fruit perforations and placed in the incubator for 24 h. D1 (200 µg/mL) was sprayed evenly on the surface of the fruit. The fruits were incubated in an incubator (25 °C, 85% relative humidity) for 96 h after inoculation with pathogens, and then the diameter of the spots was measured. Calculations were performed as follows:

$$C (\%) = [(A_{CK} - A_1) / (A_{CK} - 5)] \times 100.$$

C—control effect;

A<sub>CK</sub>—lesion diameter of the blank control group;

A<sub>1</sub>—lesion diameter after compound treatment.

C represents the control effect (%);

There were three parallel sets for each concentration, and the experiments were repeated at least twice.

### 3.6. In Vitro SDH Inhibition Assay

The succinate dehydrogenase assay kit used in the experiment was procured from Beijing Solarbio Technology Co, Beijing, China [55]. It was used to determine the inhibition of the target compound D1 against SDH in vitro, and the commercial SDHI fluopyram was used as a positive control. The newly activated bacteria were put into the sterilized PDB (Potato Dextrose Broth) medium and incubated in a constant temperature shaker (25 °C, 180 rpm/min). The drug solution was added to the above medium containing mycelium to a final concentration of 100, 50, 25 and 12.5 µg/mL and incubated in a shaker for 24 h. The mycelium was collected, freeze-dried, and ground in liquid nitrogen. Weigh 0.1 g of mycelium treated with different concentrations, assay according to the kit's instructions, set up three parallels each time, and repeat three times.

### 3.7. Molecular Docking

To further investigate whether SDH is a potential target for action, we performed molecular docking of D1 and commercially available SDHI fluopyram with SDH (PDB:2FBW) [56,57]. The experimental results were further validated at the molecular level.

### 3.8. Determination of Malondialdehyde Content

To further study the mechanism of action of these compounds, we conducted a malondialdehyde content test. Malondialdehyde (MDA) is one of the main products of membrane lipid peroxidation. Its content is usually used as an indicator of lipid peroxidation, reflecting the degree of cell membrane damage [54,58]. The MDA content detection kit used in the experiment was purchased from Beijing Soleibao Technology Co. The young viable *Phomopsis* sp. strains were selected in a sterilized PDB medium and incubated in a constant temperature shaker for 48 h. The strains were incubated in a D1 solution containing concentrations (0, 25, 50, 100, 200 µg/mL) for 24 h. Rinse the medium with sterile water, then collect the mycelium and freeze-dried. 0.1 g of mycelium treated with different concentrations of the solution was weighed separately and tested according to the

instructions of the kit. Finally, the absorbance of each sample was measured at 532 nm and 600 nm.

#### 4. Conclusions

We designed and synthesized 19 myricetin derivatives containing pyrazole-piperazinamide in this study and conducted their biological activities tests. The in vitro antibacterial experiments revealed that **D6** exhibited good inhibitory activity against *Xoo*, with an EC<sub>50</sub> value of 18.8 µg/mL. In vitro antifungal experiments demonstrated that **D16** displayed potent inhibitory activity against *P. capsici*, with an EC<sub>50</sub> value of 11.3 µg/mL. The SEM analysis showed that **D16** induced folding and curing and inhibited the growth of the *P. capsici* mycelium. Moreover, compound **D1** exhibited remarkable inhibitory effects against *Phomopsis* sp., with an EC<sub>50</sub> value of 16.9 µg/mL. The in vitro protective effect of **D1** against *Phomopsis* sp. was 74.9%, and the curative effect was 60.6%. Microscopic experiments demonstrated that **D1** inhibited mycelial growth. And **D1** can effectively inhibit the activity of SDH, and molecular docking studies confirmed its strong binding affinity with SDH protein. Additionally, **D1** increased the malondialdehyde level, leading to cell membrane damage. Based on these findings, it can be concluded that myricetin derivatives containing pyrazole piperazine amide offer new insights and a theoretical basis for developing potential fungicides.

**Supplementary Materials:** The following supporting information can be downloaded at: <https://www.mdpi.com/article/10.3390/ijms241310442/s1>.

**Author Contributions:** W.X. and F.L. conceived, designed the experiments, and wrote the manuscript; F.L., X.C. and T.Z. performed the bioactivity assays, L.X., Z.S. and H.X. analyzed the data and completed molecular docking; W.Z. assisted in the SEM; W.X. and F.L. were involved in the drafting of the manuscript and revising the manuscript. All authors have read and agreed to the published version of the manuscript.

**Funding:** This work was supported by the National Nature Science Foundation of China (No. 21867003), the Science Foundation of Guizhou Province (No. 20192452), Key Laboratory of Institute of Environment and Plant Protection (No. HZSKFKT202208).

**Institutional Review Board Statement:** Not applicable.

**Data Availability Statement:** All data generated in this study is presented in the current manuscript. No new datasets were generated. Data is available upon request from the corresponding author. Informed consent was obtained from all subjects involved in the study.

**Conflicts of Interest:** The authors declare no conflict of interest.

#### References

1. Chaudhary, P.; Singh, S.; Chaudhary, A.; Sharma, A.; Kumar, G. Overview of biofertilizers in crop production and stress management for sustainable agriculture. *Front. Plant Sci.* **2022**, *13*, 930340. [CrossRef]
2. Peng, Y.; Li, S.J.; Yan, J.; Tang, Y.; Cheng, J.P.; Gao, A.J.; Yao, X.; Ruan, J.J.; Xu, B.L. Research Progress on Phytopathogenic Fungi and Their Role as Biocontrol Agents. *Front. Microbiol.* **2021**, *12*, 670135. [CrossRef]
3. Buttner, C.; McAuliffe, O.; Ross, R.P.; Hill, C.; O'Mahony, J.; Coffey, A. Bacteriophages and bacterial plant diseases. *Front. Microbiol.* **2017**, *8*, 34. [CrossRef]
4. Ren, X.L.; Li, X.Y.; Yin, L.M.; Jiang, D.H.; Hu, D.Y. Design, Synthesis, Antiviral Bioactivity, and Mechanism of the Ferulic Acid Ester-Containing Sulfonamide Moiety. *ACS Omega* **2020**, *31*, 19721–19726. [CrossRef] [PubMed]
5. Liu, T.T.; Peng, F.; Cao, X.; Liu, F.; Wang, Q.F.; Liu, L.W.; Xue, W. Design, Synthesis, Antibacterial Activity, Antiviral Activity, and Mechanism of Myricetin Derivatives Containing a Quinazolinone Moiety. *ACS Omega* **2021**, *45*, 30826–30833. [CrossRef] [PubMed]
6. Tang, X.; Zhang, C.; Chen, M.; Xue, Y.; Liu, T.; Xue, W. Synthesis and antiviral activity of novel myricetin derivatives containing ferulic acid amide scaffolds. *New J. Chem.* **2020**, *44*, 2374–2379. [CrossRef]
7. Wei, C.; Zhao, L.; Sun, Z.; Hu, D.; Song, B. Discovery of novel indole derivatives containing dithioacetal as potential antiviral agents for plants. *Pestic. Biochem. Physiol.* **2020**, *166*, 104568. [CrossRef]
8. Roberto, N.S.; Valdirene, N.M.; Andrei, S.S.; Eriston, V.G.; Eliane, F.N.; Cirano, J.U. Trichoderma/pathogen/plant interaction in pre-harvest food security. *Fungal Biol.* **2019**, *123*, 565–583. [CrossRef]

9. Aiyim, B.T.; Ewa, W.; František, Š.; Christopher, T.E.; Dmitry, O.G. Recent advances and remaining barriers to producing novel formulations of fungicides for safe and sustainable agriculture. *J. Control. Release* **2020**, *326*, 468–481. [[CrossRef](#)]
10. Weng, C.J.; Yen, G.C. Flavonoids, a ubiquitous dietary phenolic subclass, exert extensive in vitro anti-invasive and in vivo anti-metastatic activities. *Cancer Metastasis Rev.* **2012**, *31*, 323–335. [[CrossRef](#)]
11. Bushra, S.; Farooq, A. Flavonols (kaempferol, quercetin, myricetin) contents of selected fruits, vegetables and medicinal plants. *Food Chem.* **2008**, *108*, 879–884. [[CrossRef](#)]
12. López-Lázaro, M.; Willmore, E.; Austin, C.A. The dietary flavonoids myricetin and fisetin act as dual inhibitors of DNA topoisomerases I and II in cells. *Mutat. Res.* **2010**, *696*, 41–47. [[CrossRef](#)]
13. Wang, H.F.; Keith, H. Determination of flavonols in green and black tea leaves and green tea infusions by high-performance liquid chromatography. *Food Res. Int.* **2001**, *34*, 223–227. [[CrossRef](#)]
14. Wu, Y.H.; Jiang, X.L.; Zhang, S.X.; Dai, X.L.; Liu, Y.J.; Tan, H.R.; Gao, L.P.; Xia, T. Quantification of flavonol glycosides in *Camellia sinensis* by MRM mode of UPLC-QQQ-MS/MS. *J. Chromatogr. B.* **2016**, *1017–1018*, 10–17. [[CrossRef](#)]
15. Rashed, K.; Ćirić, A.; Glamočlija, J.; Soković, M. Antibacterial and antifungal activities of methanol extract and phenolic compounds from *diospyros virginiana* L. *Ind. Crops Prod.* **2014**, *59*, 210–215. [[CrossRef](#)]
16. Yu, M.S.; Lee, J.; Lee, J.M.; Kim, Y.; Chin, Y.W.; Jee, J.G.; Keum, Y.S.; Jeong, Y.J. Identification of myricetin and scutellarein as novel chemical inhibitors of the SARS coronavirus helicase, nsP13. *Bioorg. Med. Chem. Lett.* **2012**, *22*, 4049–4054. [[CrossRef](#)]
17. Su, X.W.; D'Souza, D.H. Naturally occurring flavonoids against human norovirus surrogates. *Food Environ. Virol.* **2013**, *5*, 97–102. [[CrossRef](#)]
18. Bertin, R.; Chen, Z.; Marin, R.; Donati, M.; Feltrinelli, A.; Montopoli, M.; Zambon, S.; Manzato, E.; Frolidi, G. Activity of myricetin and other plant-derived polyhydroxyl compounds in human LDL and human vascular endothelial cells against oxidative stress. *Biomed. Pharmacother.* **2016**, *82*, 472–478. [[CrossRef](#)]
19. Qian, J.Q.; Zhang, J.Q.; Chen, Y.; Dai, C.G.; Fan, J.; Guo, H. Hypoglycemic activity and mechanisms of myricetin. *Nat. Prod. Res.* **2022**, *36*, 6177–6180. [[CrossRef](#)]
20. Liu, T.T.; Peng, F.; Zhu, Y.Y.; Cao, X.; Wang, Q.F.; Liu, F.; Liu, L.W.; Xue, W. Design, synthesis, biological activity evaluation and mechanism of action of myricetin derivatives containing thioether quinazolinone. *Arab. J. Chem.* **2022**, *15*, 1878–5352. [[CrossRef](#)]
21. Jiang, S.C.; Su, S.J.; Chen, M.; Peng, F.; Zhou, Q.; Liu, T.T.; Liu, L.W.; Xue, W. Antibacterial activities of novel dithiocarbamate-containing 4H-chromen-4-one derivatives. *J. Agric. Food Chem.* **2020**, *68*, 5641–5647. [[CrossRef](#)]
22. Jiang, S.C.; Tang, X.; Chen, M.; He, J.; Su, S.J.; Liu, L.W.; He, M.; Xue, W. Design, synthesis and antibacterial activities against *Xanthomonas oryzae* pv. *oryzae*, *Xanthomonas axonopodis* pv. *citri* and *Ralstonia solanacearum* of novel myricetin derivatives containing sulfonamide moiety. *Pest Manag. Sci.* **2020**, *76*, 853–860. [[CrossRef](#)] [[PubMed](#)]
23. Chen, M.; Tang, X.M.; Liu, T.T. Antimicrobial evaluation of myricetin derivatives containing benzimidazole skeleton against plant pathogens. *Fitoterapia* **2021**, *149*, 104804. [[CrossRef](#)] [[PubMed](#)]
24. Peng, F.; Liu, T.T.; Wang, Q.F.; Liu, F.; Cao, X.; Yang, J.S.; Liu, L.W.; Xie, C.W.; Xue, W. Antibacterial and Antiviral Activities of 1,3,4-Oxadiazole Thioether 4H-Chromen-4-one Derivatives. *J. Agric. Food Chem.* **2021**, *69*, 11085–11094. [[CrossRef](#)] [[PubMed](#)]
25. Sun, C.X.; Zhang, F.H.; Zhang, H.; Li, P.H.; Jiang, L. Design, Synthesis, Fungicidal Activity and Molecular Docking Study of Novel 2-(1-Methyl-1H-pyrazol-4-yl) pyrimidine-4-carboxamides. *Chin. J. Org. Chem.* **2022**, *42*, 0253–2786. [[CrossRef](#)]
26. Xiong, L.; Zhu, X.L.; Gao, H.W.; Fu, Y.; Hu, S.Q.; Jiang, L.N.; Yang, W.C.; Yang, G.F. Discovery of Potent Succinate-Ubiquinone Oxidoreductase Inhibitors via Pharmacophore-linked Fragment Virtual Screening Approach. *J. Agric. Food Chem.* **2016**, *64*, 4830–4837. [[CrossRef](#)]
27. Wu, J.; Song, B.A.; Hu, D.Y.; Yue, M.; Yang, S. Design, synthesis and insecticidal activities of novel pyrazole amides containing hydrazone substructures. *Pest Manag. Sci.* **2012**, *68*, 801–810. [[CrossRef](#)]
28. Shi, J.J.; Ren, G.H.; Wu, N.J.; Weng, J.Q.; Xu, T.M.; Liu, X.H.; Tan, C.X. Design, synthesis and insecticidal activities of novel anthranilic diamides containing polyfluoroalkyl pyrazole moiety. *Chin. Chem. Lett.* **2017**, *28*, 1727–1730. [[CrossRef](#)]
29. Yu, B.; Zhou, S.; Cao, L.X.; Hao, Z.S.; Yang, D.Y.; Guo, X.F.; Zhang, N.L.; Bakulev, V.; Fan, Z.J. Design, Synthesis, and Evaluation of the Antifungal Activity of Novel Pyrazole-Thiazole Carboxamides as Succinate Dehydrogenase Inhibitors. *J. Agric. Food Chem.* **2020**, *68*, 7093–7102. [[CrossRef](#)]
30. Sun, S.S.; Chen, L.; Huo, J.Q.; Wang, Y.; Kou, S.; Yuan, S.T.; Fu, Y.N.; Zhang, J.L. Discovery of Novel Pyrazole Amides as Potent Fungicide Candidates and Evaluation of Their Mode of Action. *J. Agric. Food Chem.* **2022**, *70*, 3447–3457. [[CrossRef](#)]
31. Cai, Z.F.; Zhang, W.L.; Yan, Z.J.; Du, X.H. Synthesis of Novel Pyrazole Derivatives Containing Phenylpyridine Moieties with Herbicidal Activity. *Molecules* **2022**, *27*, 6274. [[CrossRef](#)]
32. Zhang, X.J.; Wei, Z.M.; Wang, Y.J.; Yang, L.G.; Yuan, H.X.; Feng, J.T.; Gao, Y.Q.; Lei, P.; Ma, Z.Q. Synthesis and antifungal activity of 3-(difluoromethyl)-1-methylpyrazole-4-carboxylic oxime esters. *Chin. J. Pestic. Sci.* **2022**, *24*, 59–65. [[CrossRef](#)]
33. Luo, B.; Ning, Y.L. Comprehensive Overview of Carboxamide Derivatives as Succinate Dehydrogenase Inhibitors. *J. Agric. Food Chem.* **2022**, *70*, 957–975. [[CrossRef](#)]
34. Yan, Z.Z.; Liu, A.P.; Huang, M.Z.; Liu, M.H.; Pei, H.; Huang, L.; Yi, H.B.; Liu, W.D.; Hu, A.X. Design, synthesis, DFT study and antifungal activity of the derivatives of pyrazolecarboxamide containing thiazole or oxazole ring. *Eur. J. Med. Chem.* **2018**, *149*, 170–181. [[CrossRef](#)]

35. Wang, S.F.; Yin, Y.; Wu, X.; Qiao, F.; Sha, S.; Lv, P.C.; Zhao, J.; Zhu, H.L. Synthesis molecular docking and biological evaluation of coumarin derivatives containing piperazine skeleton as potential antibacterial agents. *Bioorg. Med. Chem.* **2014**, *22*, 5727–5737. [CrossRef]
36. Huang, B.S.; Kang, D.W.; Tian, Y.; Daelemans, D.; Clercq, E.; Pannecouque, C.; Zhan, P.; Liu, X.Y. Design, synthesis, and biological evaluation of piperidiny-substituted [1,2,4-triazolo[1,5-*a*]pyrimidine derivatives as potential anti-HIV-1 agents with reduced cytotoxicity. *Chem. Bio. Drug Des.* **2020**, *97*, 67–76. [CrossRef]
37. Nathans, R.; Cao, H.; Sharova, N.; Ali, A.; Sharkey, M.; Stranska, R.; Stevenson, M.; Rana, T.M. Small-molecule inhibition of HIV-1 Vif. *Nat. Biotechnol.* **2008**, *26*, 1187–1192. [CrossRef]
38. Magriotis, P. Recent progress toward the asymmetric synthesis of carbon-substituted piperazine pharmacophores and oxidative related heterocycles. *RSC Med. Chem.* **2020**, *11*, 745–759. [CrossRef]
39. Rathi, A.K.; Syed, R.; Shin, H.S.; Patel, R.V. Piperazine derivatives for therapeutic use: A patent review (2010–present). *Expert Opin. Ther. Pat.* **2016**, *26*, 777–797. [CrossRef]
40. Sun, J.; Ren, S.Z.; Lu, X.Y.; Li, J.J.; Shen, F.Q.; Xu, C.; Zhu, H.L. Discovery of a series of 1,3,4-oxadiazole-2(3*H*)-thione derivatives containing piperazine skeleton as potential fak inhibitors. *Bioorg. Med. Chem.* **2017**, *25*, 2593–2600. [CrossRef]
41. Xue, W. Preparation Methods and Applications of Pyrazole Amides and Pyrazolimide Derivatives Containing Substituted 1,3,4-Thiadiazole Thioethers: China, 201410175919.4. 30 July 2014. Available online: <https://pss-system.cponline.cnipa.gov.cn/documents/detail?prevPageTit=changgui> (accessed on 15 February 2023).
42. Dai, H.; Li, Y.Q.; Du, D.; Qin, X.; Zhang, X.; Yu, H.B.; Fang, J.X. Synthesis and Biological Activities of Novel Pyrazole Oxime Derivatives Containing a 2-Chloro-5-thiazolyl Moiety. *J. Agric. Food Chem.* **2008**, *56*, 10805–10810. [CrossRef] [PubMed]
43. Fang, H.B.; Chen, Z.F.; Hua, X.W.; Liu, W.R.; Xue, C.M.; Liu, Y.; Zhu, X.H.; Yuan, M.; Cheng, S.; Bazhanau, D.; et al. Synthesis and biological activity of amide derivatives derived from natural product Waltherione F. *Med. Chem. Res.* **2022**, *31*, 485–496. [CrossRef]
44. Peng, F.; Liu, T.T.; Cao, X.; Wang, Q.F.; Liu, F.; Liu, L.W.; He, M.; Xue, W. Antiviral Activities of Novel Myricetin Derivatives Containing 1,3,4-Oxadiazole Bisthioether. *Chem. Biodivers.* **2021**, *19*, 1612–1872. [CrossRef] [PubMed]
45. Chen, Y.; Li, P.; Su, S.J.; Chen, M.; He, J.; Liu, L.W.; He, M.; Wang, H.; Xue, W. Synthesis and antibacterial and antiviral activities of myricetin derivatives containing a 1,2,4-triazole Schiff base. *RSC Adv.* **2019**, *9*, 23045–23052. [CrossRef]
46. He, J.; Tang, X.M.; Liu, T.T.; Peng, F.; Zhou, Q.; Liu, L.W.; He, M.; Xue, W. Synthesis and antibacterial activity of novel myricetin derivatives containing sulfonylpiperazine. *Chem. Pap.* **2021**, *75*, 1021–1027. [CrossRef]
47. Tang, X.M.; Zhou, Q.; Zhan, W.L.; Hu, D.; Zhou, R.; Sun, N.; Chen, S.; Wu, W.N.; Xue, W. Synthesis of novel antibacterial and antifungal quinoxaline derivatives. *RSC Adv.* **2022**, *12*, 2399–2407. [CrossRef]
48. Su, S.J.; Zhou, Q.; Tang, X.M.; Peng, F.; Liu, T.T.; Liu, L.W.; Xie, C.W.; He, M.; Xue, W. Design, synthesis, and antibacterial activity of novel myricetin derivatives containing sulfonate. *Monatsh. Chem.* **2021**, *152*, 345–356. [CrossRef]
49. Guo, T.; Xia, R.J.; Liu, T.T.; Peng, F.; Tang, X.; Zhou, Q.; Luo, H.; Xue, W. Synthesis, Biological Activity and Action Mechanism Study of Novel Chalcone Derivatives Containing Malonate. *Chem. Biodivers.* **2020**, *17*, e2000025. [CrossRef]
50. Wu, H.B.; Guo, P.X.; Ma, L.H.; Li, X.M.; Liu, T.T. Nematicidal, antifungal and insecticidal activities of *Artemisia halodendron* extracts: New polyacetylenes involved. *Ind. Crops Prod.* **2021**, *170*, 113825. [CrossRef]
51. Zhang, J.; Han, R.Y.; Ye, H.C.; Zhou, Y.; Zhang, Z.K.; Yuan, E.L.; Li, Y.; Yan, C.; Liu, X.; Feng, G.; et al. Effect of pseudolaric acid B on biochemical and physiologic characteristics in *Colletotrichum gloeosporioides*. *Pestic. Biochem. Phys.* **2018**, *147*, 75–82. [CrossRef]
52. Wang, X.B.; Chai, J.Q.; Kong, X.Y.; Jin, F.; Chen, M.; Yang, C.L.; Xue, W. Expedient discovery for novel antifungal leads: 1,3,4-Oxadiazole derivatives bearing a quinazolin-4(3*H*)-one fragment. *Bioorg. Med. Chem.* **2021**, *45*, 116330. [CrossRef]
53. Zhou, Y.; Gong, G.S.; Cui, Y.L.; Zhang, D.X.; Chang, X.L.; Hu, R.P.; Liu, N.; Sun, X.F. Identification of Botryosphaeriaceae Species Causing Kiwifruit Rot in Sichuan Province. *Plant Dis.* **2015**, *99*, 699–708. [CrossRef]
54. Zhou, R.; Zhan, W.; Yuan, C.; Zhang, T.; Mao, P.; Sun, Z.; An, Y.; Xue, W. Design, Synthesis and Antifungal Activity of Novel 1,4-Pentadiene-3-one Containing Quinazolinone. *Int. J. Mol. Sci.* **2023**, *24*, 2599. [CrossRef] [PubMed]
55. Long, Z.Q.; Yang, L.L.; Zhang, J.R.; Liu, S.T.; Xie, J.; Wang, P.Y.; Zhu, J.J.; Shao, W.B.; Liu, L.W.; Yang, S. Fabrication of Versatile Pyrazole Hydrazone Derivatives Bearing a 1,3,4-Oxadiazole Core as Multipurpose Agricultural Chemicals against Plant Fungal, Oomycete, and Bacterial Diseases. *J. Agric. Food Chem.* **2021**, *69*, 8380–8393. [CrossRef] [PubMed]
56. Peng, F.; Liu, T.T.; Zhu, Y.Y.; Liu, F.; Cao, X.; Wang, Q.F.; Liu, L.W.; Xue, W. ‘Novel 1,3,4-oxadiazole sulfonate/carboxylate flavonoid derivatives: Synthesis and biological activity’. *Pest Manag. Sci.* **2022**, *79*, 274–283. [CrossRef] [PubMed]
57. Wang, X.B.; Wang, A.; Qiu, L.L.; Chen, M.; Lu, A.M.; Li, G.H.; Yang, C.L.; Xue, W. Expedient Discovery for Novel Antifungal Leads Targeting Succinate Dehydrogenase: Pyrazole-4-formylhydrazide Derivatives Bearing a Diphenyl Ether Fragment. *J. Agric. Food Chem.* **2020**, *68*, 14426–14437. [CrossRef]
58. Zafari, M.; Ebadi, A.; Jahanbakhsh, S.; Sedghi, M. Safflower (*Carthamus tinctorius*) Biochemical Properties, Yield, and Oil Content Affected by 24-Epibrassinosteroid and Genotype under Drought Stress. *J. Agric. Food. Chem.* **2020**, *68*, 6040–6047. [CrossRef]

**Disclaimer/Publisher’s Note:** The statements, opinions and data contained in all publications are solely those of the individual author(s) and contributor(s) and not of MDPI and/or the editor(s). MDPI and/or the editor(s) disclaim responsibility for any injury to people or property resulting from any ideas, methods, instructions or products referred to in the content.